

Resonance perfect absorption by exciting hyperbolic phonon polaritons in 1D hBN gratings

BO ZHAO^{1,2,3} AND ZHUOMIN M. ZHANG^{1,4}

¹*G.W. Woodruff School of Mechanical Engineering, Georgia Institute of Technology, Atlanta, Georgia 30332, USA*

²*Current address: Department of Electrical Engineering, Ginzton Laboratory, Stanford University, Stanford, California 94305, USA*

³*bzhao35@gatech.edu*

⁴*zhuomin.zhang@me.gatech.edu*

Abstract: Natural materials with hyperbolic responses can confine light with well-defined propagation directions inside the micro/nanostructure. Here we theoretically demonstrate that strong resonance absorption can be achieved in one-dimensional gratings made of hexagonal boron nitride (hBN) due to hyperbolic phonon polaritons. The radiative properties of both trapezoidal and square resonators are calculated using anisotropic rigorous coupled-wave analysis. The resonance wavelengths can be theoretically predicted and are shown to follow the anomalous or traditional scaling laws depending on the hyperbolicity. These findings may benefit the applications including photodetection, color filters, and optomechanics.

© 2017 Optical Society of America

OCIS codes: (050.2770) Gratings; (260.5740) Resonance.

References and links

1. F. Bonaccorso, Z. Sun, T. Hasan, and A. Ferrari, "Graphene photonics and optoelectronics," *Nat. Photonics* **4**(9), 611–622 (2010).
2. K.-S. Lee and M. A. El-Sayed, "Gold and silver nanoparticles in sensing and imaging: sensitivity of plasmon response to size, shape, and metal composition," *J. Phys. Chem. B* **110**(39), 19220–19225 (2006).
3. H. Zhu, F. Yi, and E. Cubukcu, "Plasmonic metamaterial absorber for broadband manipulation of mechanical resonances," *Nat. Photonics* **10**(11), 709–714 (2016).
4. M. S. Tame, K. R. McEnery, S. K. Ozdemir, J. Lee, S. A. Maier, and M. S. Kim, "Quantum plasmonics," *Nat. Phys.* **9**(6), 329–340 (2013).
5. J. Pérez-Juste, I. Pastoriza-Santos, L. M. Liz-Marzán, and P. Mulvaney, "Gold nanorods: Synthesis, characterization and applications," *Coord. Chem. Rev.* **249**(17–18), 1870–1901 (2005).
6. P. K. Jain, K. S. Lee, I. H. El-Sayed, and M. A. El-Sayed, "Calculated Absorption and Scattering Properties of Gold Nanoparticles of Different Size, Shape, and Composition: Applications in Biological Imaging and Biomedicine," *J. Phys. Chem. B* **110**(14), 7238–7248 (2006).
7. B. Zhao and Z. M. Zhang, "Study of magnetic polaritons in deep gratings for thermal emission control," *J. Quant. Spectrosc. Radiat. Transf.* **135**, 81–89 (2014).
8. B. Zhao and Z. M. Zhang, "Strong Plasmonic Coupling between Graphene Ribbon Array and Metal Gratings," *ACS Photonics* **2**(11), 1611–1618 (2015).
9. H. Wang and L. Wang, "Perfect selective metamaterial solar absorbers," *Opt. Express* **21**(S6 Suppl 6), A1078–A1093 (2013).
10. N. I. Landy, S. Sajuyigbe, J. J. Mock, D. R. Smith, and W. J. Padilla, "Perfect Metamaterial Absorber," *Phys. Rev. Lett.* **100**(20), 207402 (2008).
11. L. Ferrari, C. Wu, D. Lepage, X. Zhang, and Z. Liu, "Hyperbolic metamaterials and their applications," *Prog. Quantum Electron.* **40**, 1–40 (2015).
12. X. Yang, J. Yao, J. Rho, X. Yin, and X. Zhang, "Experimental realization of three-dimensional indefinite cavities at the nanoscale with anomalous scaling laws," *Nat. Photonics* **6**(7), 450–454 (2012).
13. X. G. Xu, B. G. Ghamsari, J.-H. Jiang, L. Gilburd, G. O. Andreev, C. Zhi, Y. Bando, D. Golberg, P. Berini, and G. C. Walker, "One-dimensional surface phonon polaritons in boron nitride nanotubes," *Nat. Commun.* **5**, 4782 (2014).
14. J. D. Caldwell, A. V. Kretinin, Y. Chen, V. Giannini, M. M. Fogler, Y. Francescato, C. T. Ellis, J. G. Tischler, C. R. Woods, A. J. Giles, M. Hong, K. Watanabe, T. Taniguchi, S. A. Maier, and K. S. Novoselov, "Sub-diffractive volume-confined polaritons in the natural hyperbolic material hexagonal boron nitride," *Nat. Commun.* **5**, 5221 (2014).

15. P. Li, M. Lewin, A. V. Kretinin, J. D. Caldwell, K. S. Novoselov, T. Taniguchi, K. Watanabe, F. Gaussmann, and T. Taubner, "Hyperbolic phonon-polaritons in boron nitride for near-field optical imaging and focusing," *Nat. Commun.* **6**, 7507 (2015).
16. Z. Sun, Á. Gutiérrez-Rubio, D. N. Basov, and M. M. Fogler, "Hamiltonian Optics of Hyperbolic Polaritons in Nanogranules," *Nano Lett.* **15**(7), 4455–4460 (2015).
17. S. Dai, Z. Fei, Q. Ma, A. S. Rodin, M. Wagner, A. S. McLeod, M. K. Liu, W. Gannett, W. Regan, K. Watanabe, T. Taniguchi, M. Thieme, G. Dominguez, A. H. Castro Neto, A. Zettl, F. Keilmann, P. Jarillo-Herrero, M. M. Fogler, and D. N. Basov, "Tunable Phonon Polaritons in Atomically Thin Van Der Waals Crystals of Boron Nitride," *Science* **343**(6175), 1125–1129 (2014).
18. S. Dai, Q. Ma, T. Andersen, A. S. McLeod, Z. Fei, M. K. Liu, M. Wagner, K. Watanabe, T. Taniguchi, M. Thieme, F. Keilmann, P. Jarillo-Herrero, M. M. Fogler, and D. N. Basov, "Subdiffractional focusing and guiding of polaritonic rays in a natural hyperbolic material," *Nat. Commun.* **6**, 6963 (2015).
19. Z. M. Zhang, *Nano/Microscale Heat Transfer* (McGraw-Hill, New York, 2007).
20. A. Kumar, T. Low, K. H. Fung, P. Avouris, and N. X. Fang, "Tunable Light-Matter Interaction and the Role of Hyperbolicity in Graphene-hBN System," *Nano Lett.* **15**(5), 3172–3180 (2015).
21. B. Zhao and Z. M. Zhang, "Perfect mid-infrared absorption by hybrid phonon-plasmon polaritons in hBN/metal-grating anisotropic structures," *Int. J. Heat Mass Transfer* **106**, 1025–1034 (2017).
22. B. Zhao, J. M. Zhao, and Z. M. Zhang, "Resonance enhanced absorption in a graphene monolayer using deep metal gratings," *J. Opt. Soc. Am. B* **32**(6), 1176–1185 (2015).
23. A. J. Giles, S. Dai, O. J. Glembocki, A. V. Kretinin, Z. Sun, C. T. Ellis, J. G. Tischler, T. Taniguchi, K. Watanabe, M. M. Fogler, K. S. Novoselov, D. N. Basov, and J. D. Caldwell, "Imaging of Anomalous Internal Reflections of Hyperbolic Phonon-Polaritons in Hexagonal Boron Nitride," *Nano Lett.* **16**(6), 3858–3865 (2016).
24. A. Alù, M. G. Silveirinha, A. Salandrino, and N. Engheta, "Epsilon-near-zero metamaterials and electromagnetic sources: Tailoring the radiation phase pattern," *Phys. Rev. B* **75**(15), 155410 (2007).
25. E. E. Narimanov and A. V. Kildishev, "Metamaterials: Naturally hyperbolic," *Nat. Photonics* **9**(4), 214–216 (2015).
26. P. Li, I. Dolado, F. J. Alfaro-Mozaz, A. Y. Nikitin, F. Casanova, L. E. Hueso, S. Vélez, and R. Hillenbrand, "Optical nanoimaging of hyperbolic surface polaritons at the edges of van der Waals materials," *Nano Lett.* **17**(1), 228–235 (2017).
27. Z. Jacob and E. E. Narimanov, "Optical hyperspace for plasmons: Dyakonov states in metamaterials," *Appl. Phys. Lett.* **93**(22), 221109 (2008).
28. O. Takayama, D. Artigas, and L. Torner, "Practical Dyakonons," *Opt. Lett.* **37**(20), 4311–4313 (2012).

1. Introduction

Resonance absorption plays an important role in many applications such as optoelectronics, chemical sensing, optomechanics, and quantum optics [1–4]. By confining light within the resonators of miniaturized sizes, one can increase the photon density of states and thus enhance the light-matter interaction to achieve strong resonance absorption. Examples of this nature include nanoparticles of different shapes [5,6], gratings that support localized resonances [7–9], and surfaces with metamaterial resonators [10]. Another approach is to utilize hyperbolic metamaterials, such as metal-dielectric multilayers and nanowire array, whose isofrequency surface can extend to infinity such that waves with large wave vectors are allowed to propagate inside the material [11]. Resonators made of hyperbolic metamaterials thus can confine light in a scale smaller than the diffraction limit [12]. However, the maximum allowed wavevector is limited by the size of the unit cell of the metamaterials for the sake of the validity of effective medium approximation [11]. This in turn hinders the degree of confinement of light inside artificial hyperbolic metamaterials.

One of the solutions is to use natural hyperbolic materials such as hexagonal boron nitride (hBN), which possesses two hyperbolic regions in the mid-infrared range with different hyperbolicities. Since the unit cell of these materials is at the atomic scale, an extremely high degree of confinement can be achieved [13–16]. It has been experimentally demonstrated that hyperbolic phonon polaritons (HPPs) can be supported by an hBN film with a thickness that is only several nanometers [17]. Therefore, resonators made of hBN may enable highly concentrated strong resonance absorption. More interestingly, due to the extreme confinement, the propagation of HPPs is highly directional and can be well described based on the dielectric function of hBN [15, 18]. This unique property of HPPs has attracted significant attention because of the potential applications in sub-diffraction imaging and

focusing [15, 18]. However, using HPPs to create resonance absorption has not yet been explored and hyperbolic gratings may provide another way to create strong absorption.

In this work, we theoretically demonstrate that perfect or nearly perfect absorption can be achieved with hBN resonators due to different resonant modes. The frequency of the resonance modes can be well predicted based on the propagation direction of HPPs and the geometry of the resonators. Resonance modes with higher orders may oscillate at a higher or lower frequency, depending on which hyperbolic region the resonance occurs.

2. Strong resonance absorption

A 1D trapezoidal hBN grating over a Ag film (substrate) is illustrated in Fig. 1(a). The grating is periodic in the x -direction with a period of Λ . In each period, hBN is shaped to an isosceles trapezoid with its height, short and long bases being h , t_t , and t_b , respectively. The dielectric function of Ag is obtained using a Drude model [7, 19]. Incident plane waves have an incidence angle θ and a wavevector $\mathbf{k}_{\text{inc}} = k_0 \sin \theta \hat{\mathbf{x}} + k_0 \cos \theta \hat{\mathbf{z}}$, where k_0 is the magnitude of the wavevector in vacuum. The plane of incidence is the x - z plane and the incident waves are transverse-magnetic (TM) polarized with the magnetic field oscillating in the y -direction. The right-side trapezoid also shows HPP propagation to be discussed later. The optical property of hBN is described by a tensor, $\hat{\epsilon}_{\text{hBN}} = \text{diag}(\epsilon_{\perp}, \epsilon_{\perp}, \epsilon_{\parallel})$, with the optical axis in the z -direction in the given coordinate [20]. The real and imaginary parts of the dielectric function are respectively denoted as ϵ' and ϵ'' hereafter. The phonon modes of hBN result in a Type-II hyperbolic region ($\epsilon'_{\perp} < 0$ and $\epsilon'_{\parallel} > 0$) from about $6.2 \mu\text{m}$ to $7.3 \mu\text{m}$ and a Type-I hyperbolic region ($\epsilon'_{\perp} > 0$ and $\epsilon'_{\parallel} < 0$) from $12 \mu\text{m}$ to $12.8 \mu\text{m}$, respectively. In this work, we focus on the Type-II hyperbolic region but the discussed findings are also applicable in the Type-I region. The absorptance is obtained by one minus the reflectance. Anisotropic rigorous coupled-wave analysis is employed to calculate the reflectance and field distributions [21]. The grating is discretized using 100 layers in a stairwise manner.

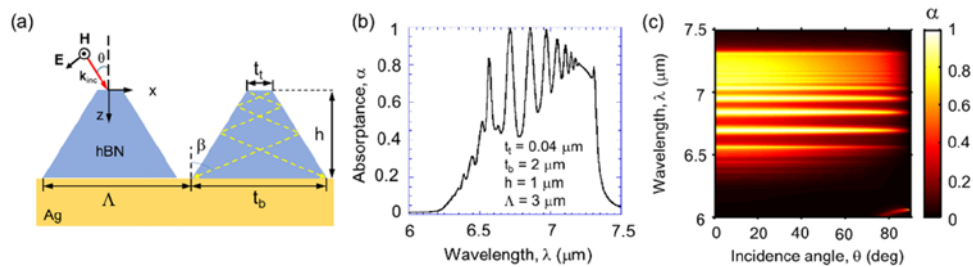


Fig. 1. (a) Schematic of the proposed structure with hBN trapezoidal gratings on a Ag substrate. The right-side structure also shows the propagation of HPPs. (b) The absorptance spectrum for TM waves at normal incidence ($\theta = 0^\circ$) of the structure shown in (a) with the grating parameters given in the figure. (c) Angular dependence of the resonance absorptance of the same structure.

Figure 1(b) shows the absorption spectrum of the structure when $\Lambda = 3 \mu\text{m}$, $t_t = 0.04 \mu\text{m}$, $t_b = 2 \mu\text{m}$, and $h = 1 \mu\text{m}$. Several strong absorption peaks occur within the Type-II hyperbolic region. The first five predominate peaks are at $\lambda = 6.56 \mu\text{m}$, $6.72 \mu\text{m}$, $6.85 \mu\text{m}$, $6.97 \mu\text{m}$, and $7.05 \mu\text{m}$ with the absorptance (α) being 0.83, 1.0, 1.0, 0.99, and 0.94, respectively. The high absorptance indicates a strong light-matter interaction. Note that the highly reflecting silver substrate is critical to the strong absorption in the hBN gratings, and the absorptance would decrease if a transparent substrate were used. The resonances are insensitive to the change of incidence angle as illustrated by the contour plot shown in Fig. 1(c), and more explanations will be given later. To demonstrate the nature of the resonances, the local power

dissipation, $w(x, z) = 0.5\varepsilon_0\omega(\varepsilon_{\perp}''|E_x|^2 + \varepsilon_{\parallel}''|E_z|^2)$ with ε_0 and ω respectively being the vacuum permittivity and angular frequency, is calculated at the first, third, and fifth predominant absorptance peak, as shown in Fig. 2(a), (b), and (c), respectively [21, 22]. Almost all the absorbed power is dissipated inside the hBN resonators. Thus the coupling between the adjacent trapezoids can be neglected and each of the trapezoids acts as an individual resonator. It is clear that some straight bright rays show up inside the hBN trapezoid, indicating a highly localized strong absorption. They are caused by HPPs as will be discussed in the next.

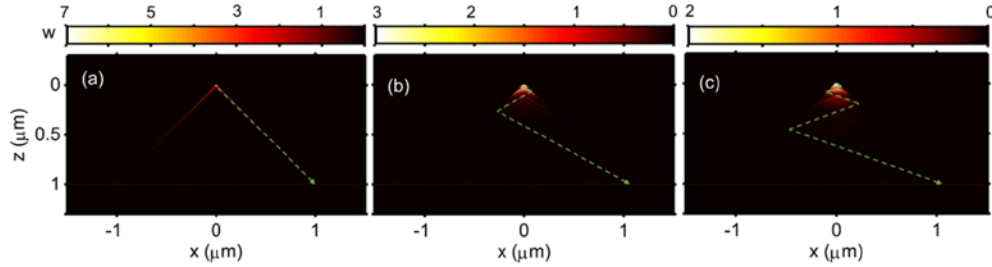


Fig. 2. Local power dissipation contours in the structure for (a) $\lambda = 6.56 \mu\text{m}$; (b) $\lambda = 6.86 \mu\text{m}$; and (c) $\lambda = 7.05 \mu\text{m}$. The dashed line with an arrow shows the directional propagation of HPPs (one branch) inside the trapezoidal resonator whose geometry is the same as for Fig. 1(b). The incidence electric field is 1 V/m and the unit for w is 10^5 W/m^3 . The white dashed line shows the interface below which is the Ag substrate.

3. Hyperbolic phonon polaritons (HPPs)

For TM waves, the hyperbolic regions allow waves with unbounded wavevectors to propagate as can be seen from the isofrequency curve $k_x^2/\varepsilon_{\parallel} + k_z^2/\varepsilon_{\perp} = k_0^2$, where $\mathbf{k} = (k_x, k_z)$ represents the allowed wave vector. Since the allowed wave vectors follow a hyperbola, both k_x and k_z can extend to very large values that are limited only by the atomic distances between hBN monolayers. It has been demonstrated theoretically and experimentally that an hBN film can support multiple orders of HPPs with wavevectors that can extend to more than $100k_0$. The large wavevectors make the isofrequency curve approach the asymptotic lines described by $k_z = \pm\sqrt{-\varepsilon_{\perp}/\varepsilon_{\parallel}}k_x$, and thus the propagation angle of the HPPs, defined as the angle between z -axis and the energy flux of the polaritons, is almost independent of the wavevectors and can be described as [14, 15, 18]

$$\beta = \arctan\left(\sqrt{\frac{\varepsilon_{\perp}}{\varepsilon_{\parallel}}}\right) \quad (1)$$

This formula provides a way to calculate the propagation angle of HPPs at any given wavelength.

For the trapezoid resonators, the dissipation toward the top is stronger as shown in Fig. 2, indicating a concentrated electric field therein. Due to local scattering, concentrated electric field with high wavevectors are generated near the edge of trapezoid [14], and HPPs are launched predominantly from the two upper edges, resulting in polariton rays with strong dissipation. This can be justified by a close analysis on the direction of the strips, which agrees well with the propagation angle of the HPPs predicted by Eq. (1). The HPPs experience total internal reflections on the sides, and based on the field plots, they end at the bottom corner of the trapezoid to form a resonance. The dashed lines indicate one of the two paths that HPPs follow. The resonance conditions can be predicted based on this picture by considering the right-side resonator shown in Fig. 1(a). The dashed lines show the two

branches of HPPs. Note that the reflection of the HPPs on the sides of the trapezoid are not specular but anomalous, meaning that the reflection of HPPs are not affected by the slope of the sides and the polaritons reflect as if the sides are vertical, as has been experimentally justified in a similar cone nanostructure [23]. Based on Eq. (1), one can obtain the order of the resonances, which equals the number of reflections HPPs experience on the sides:

$$n = \frac{\ln(t_t/t_b)}{\ln\left(\frac{2h \tan \beta - t_b + t_t}{2h \tan \beta + t_b - t_t}\right)} \quad (2)$$

Since propagation angle β depends on wavelength, only at a specific wavelength can the right-hand-side take integer values, yielding a way to predict the resonance conditions. Based on this method, the predicted wavelengths for the first five orders (i.e. $n = 1$ to 5) are 6.56 μm , 6.68 μm , 6.83 μm , 6.95 μm , and 7.03 μm , matching well with the simulation and justifying that the resonances are caused by the directional propagation of HPPs. The three resonances shown in Fig. 2 are thus the first three odd orders.

Since the resonances are localized, they are insensitive to the change of incidence angle because of the spatial incoherence, as demonstrated previously in Fig. 1(c). Note that in the Type-II hyperbolic region, β increases as the wavelength becomes longer [15]. Thus, the resonances associated with lower orders are excited at shorter wavelengths. This is very different from traditional cavity resonances and a similar anomalous scaling law was demonstrated in a metal-dielectric multilayer hyperbolic metamaterials [12]. However, since the propagation direction of the polaritons can only be wave vector independent when extreme confinement is supported, the resonance in hyperbolic metamaterial resonators can hardly be analyzed using HPPs or similar polaritons like the case discussed here. Moreover, similar resonance effect is supported between 12 μm to 12.8 μm in Type-I hyperbolic region [14], though not shown here. In this region, however, β decreases as the wavelength becomes longer, and thus resonators show traditional scaling law.

One may have noticed that the absorptance between 6.2 μm to 6.5 μm is not high. It is because the base angle of the considered trapezoid is 45.6°, and HPPs initiated from the top corners have to possess a propagation angle larger than this value to propagate inside the resonator. Thus, λ needs to be longer than about 6.5 μm , at which $\beta = 45.6^\circ$, to form a resonance inside the resonator, indicating that one may manipulate the shape of the resonator to tune the absorptance spectrum. Figure 3(a) displays the absorptance of an hBN grating with $\Lambda = 3 \mu\text{m}$ and $h = t_t = t_b = 2 \mu\text{m}$. In this case, the hBN grating strips have square cross sections. The resonance peaks can be clearly identified. The local power dissipation contours for the three dominant peaks at $\lambda = 6.29 \mu\text{m}$, 6.41 μm , and 6.56 μm are displayed in Fig. 3(b). The resonance peak at $\lambda = 7.32 \mu\text{m}$ is possibly caused by the epsilon-near-zero mode [24] since it is close to the edge of the hyperbolic region. The square resonators show Fabry-Pérot-like resonances. The order of the resonances can be denoted as (m,n) , where m and n represent the resonance order in the x - and z -directions, respectively. Under this convention, the previously discussed resonances in trapezoid shape can be denoted as $(1,n)$. The orders of the three resonances can be identified as (3,1), (3,2), and (3,3), respectively. In order to form such a resonance, the direction of the HPPs for resonance (m,n) needs to satisfy

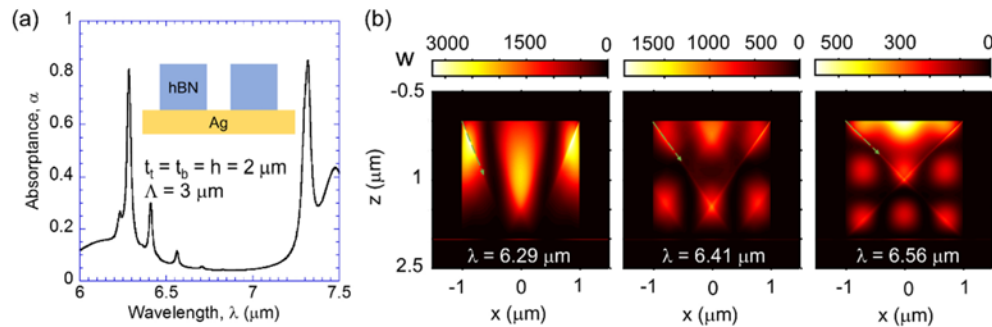


Fig. 3. (a) Normal absorbance of an hBN grating with a square cross section for TM waves. The insert is a schematic of the structure with the geometric parameters indicated on the figure. (b) Power dissipation contours at three resonance wavelengths $\lambda = 6.29 \mu\text{m}$, $\lambda = 6.41 \mu\text{m}$ and $\lambda = 6.56 \mu\text{m}$. The unit of w is W/m^3 , and the dashed line with an arrow w shows the directional propagation of HPPs.

$$\tan \beta = \frac{n}{m} \quad (3)$$

Based on this equation, the wavelengths of the three resonances are obtained as $\lambda = 6.27 \mu\text{m}$, $6.39 \mu\text{m}$, and $6.55 \mu\text{m}$, respectively, which agree well with the simulation. Note that Eq. (3) does not contain any geometric parameters of the resonator, indicating a possibility to create rectangular resonators with similar shapes but different dimensions that can resonate at the same wavelength. Since materials with natural hyperbolicity or intrinsic hyperbolic dispersion are accessible from the visible to the microwave range [25], similar hyperbolic resonators may be designed in different wavelength ranges. It should be noted that hyperbolic surface polaritons or Dyakonov plasmons [26–28] can also be supported by hBN when the optic axis lies in plane of the interface. A careful analysis of the field plots suggests that the discussed resonances in hBN grating are caused by bulk polaritons instead of surface waves. The hyperbolic surface polaritons may worth further explorations for their potentials to create resonance absorption.

4. Conclusions

In conclusion, this work demonstrates that hyperbolic materials such as hBN can be used to build resonators with wavelength-selective absorption and the absorption peak can reach unity. The resonances are caused by the directional propagation of HPPs, and the resonance wavelength can be well correlated to the shape of the resonator. Different resonators with the same shape but different sizes may be designed to resonate at the same frequencies. This methodology may be used to design resonators made of natural hyperbolic materials in different frequency ranges for applications such as photodetection, optical filters, optomechanical sensors, and energy harvesting.

Funding

National Science Foundation (NSF) (CBET-1603761).